Available online at www.sciencedirect.com

ScienceDirect

Solar Energy 100 (2014) 203–216

SOLAR ENERGY

www.elsevier.com/locate/solener

Evaluation of hourly solar radiation on inclined surfaces at Seoul by Photographical Method

Kapchun Yoon [a,1], Gyeong Yun [a,1], Jongug Jeon [b,2], Kang Soo Kim [a,*]

[a] Dept. of Architecture, Korea University, 5-1 Anam-dong, Seongbuk-gu 136-713, South Korea

[b] Korea Refrigeration & Air-conditioning Assessment Center (KRAAC), 41-14 Barangondan-ro, Hyangnam-eup, Hwaseong-si, Gyeonggi-do 445-938, South Korea

Received 3 July 2013; received in revised form 11 November 2013; accepted 14 November 2013
Available online 31 December 2013

Communicated by: Associate Editor Jan Kleissl

Abstract

Generally, a proper solar radiation model considers nothing more than the angle of inclination of a slope, without considering the influence of obstacles and surrounding buildings. In this study, we proposed a Photographical Method, which can increase the prediction accuracy of solar radiation on an inclined surface, with considering the shape of obstacles in the sky view. This paper evaluated twenty cases (5 solar radiation models in each of 4 albedo models), by the new method of the Photographical Method (PM). The following conclusions were drawn: (1) The prediction accuracy of solar radiation on an inclined surface was improved in all twenty cases with the PM. (2) The new method showed a higher degree of improvement of prediction accuracy in the low range of solar radiation (a high proportion of diffuse solar radiation). (3) The prediction accuracy of solar radiation with the PM improves with increasing tilt angle from the horizontal to the vertical. Applying the Photographical Method is more suited to an urban region with a forest of buildings, than a region of wide grasslands and sunny climate.

Keywords: Solar radiation; Inclined surface; Photographical Method; Empirical validation

1. Introduction

The accurate calculation of solar radiation on an inclined surface is very important in many practical applications of solar energy, such as the calculation of the heating and cooling energy use of buildings, the evaluation of photovoltaic plants, BIPV, and so on. Therefore, various prediction models have been proposed to estimate the amount of global and diffuse solar radiation on an inclined surface, for example those of Liu and Jordan (1963), Hay and Davies (1980), Reindl et al. (1990) and Perez et al. (1990), among many others.

Many researchers evaluated several prediction models. Kambezidis et al. (1994) compared the hourly radiation value with twelve sky diffuse models and four albedo models, and found an accurate combined model for Greece (Latitude: 37.98°N, Longitude: 23.75°E). In doing so, he asserts that the Perez model, (which has generally been considered as the most accurate model), is not accurate in every region, and maintains that there exists a most appropriate model for each region.

Vartiainen (2000) combined five solar radiation models and six sky distribution models with twenty-four inclined surfaces for Finland (Latitude: 60°27′N, Longitude: 22°18′E). Cucumo et al. (2007) compared the hourly radiation data calculated by various calculation models of

* Corresponding author. Tel.: +82 10 8862 3052; fax: +82 2 921 7947.
E-mail addresses: kapchun@korea.ac.kr (K. Yoon), poprin@korea.ac.kr (G. Yun), jujeon@kraac.or.kr (J. Jeon), kskim@korea.ac.kr (K.S. Kim).
[1] Tel.: +82 2 3290 3744; fax: +82 2 921 7947.
[2] Tel.: +82 31 8047 0364; fax: +82 31 8047 0393.

0038-092X/$ - see front matter © 2013 Elsevier Ltd. All rights reserved.
http://dx.doi.org/10.1016/j.solener.2013.11.011

Nomenclature

I	global solar radiation on inclined surface, W/m^2
I_{DN}	direct normal solar radiation, W/m^2
I_{dH}	diffuse horizontal solar radiation, W/m^2
I_{GH}	global horizontal solar radiation, W/m^2
I_O	extraterrestrial direct normal solar radiation, W/m^2
SVF	sky view factor, –
GVF	ground view factor, –
K	anisotropic index, –
i	incidence angle of sun's rays on inclined surface, °
H	Gueymard's solar incidence angle on inclined surface, $0.01(90 - i)$ °
a_0, a_1, a_2, a_3	Gueymard's monthly basis coefficients of average ground reflectance, –
A	NKemdirim's coefficient of crop factor, –
B	NKemdirim's coefficient of slope factor, –
f_{bs}	Gueymard's shadow factor for direct solar radiation, –
f_{af}	Gueymard's anisotropy coefficient for forward augmented reflection, –
f_{ab}	Gueymard's anisotropy coefficient for backward augmented reflection, –
a, b	Perez's incidence angle of the sun and surface coefficients, –
F_1	Perez's circumsolar coefficient, –
F_2	Perez's horizon brightening coefficient, –
R	radiance distribution index, –

Greek symbols

ρ	ground reflectance, –
α	solar azimuth angle relative to the inclined surface, °
Ø	latitude angle, °
θ_z	solar zenith angle, °
β	surface tilt angle from horizon, °
ρ_b	ground reflectance for direct solar radiation, –
ρ_d	ground reflectance for diffuse solar radiation, –
ρ_n	ground reflectance for purely isotropic reflection, –

south, west, north and east aspect, measured at Arcavacata di Rende (Latitude: 39°18′N, Longitude: 16°15′E), and found the most accurate model. These studies revealed that even in the same region, solar radiation model accuracy was found to be different, depending on the direction and slope.

Loutzenhiser et al. (2007) compared daily solar radiation at a vertical surface (Latitude: 47°24′N, Longitude: 8°36′E) by seven prediction models that made wide use of building energy simulation codes. He informed and analyzed all solar radiation models in building energy simulation programs, such as ENERGYPLUS, DOE, ESP-r and TRNSYS.

Other studies have been carried out in Saudi Arabia (Latitude: 21°42′N, Longitude: 39°11′E) (el-Sebaii et al., 2010), Spain (Latitude: 41°49′N, Longitude: 4°56′E) (Diez-Mediavilla et al., 2005), and Greece (Latitude: 37°59′N, Longitude: 23°45′E) (Kambezidis et al., 1994). Many studies have been performed in various locations with the changing of variables, such as the ground reflectance model, sky distribution model, and climate, surface direction, and so on.

In this paper, we assumed that the accuracy of the estimated results from the optimal solar radiation model could be affected by the view of the environment, and an obstacle's shape.

Generally, the proper solar radiation model was suggested by using the measured data from a wide field or the top of a mountain, to avoid the shielding effect of obstacles. Therefore, the solar radiation model considers no more than the angle of inclination of the slope, without considering the effect of obstacles and surrounding buildings. It quickly becomes apparent that the predicted radiation from conventional methods cannot give accurate results, due to the difference of the sky view factor caused by obstacles and surrounding buildings.

This study includes the following processes.

1. Predict solar radiation on an inclined surface, by combining five existing solar radiation models, and four ground reflectance models.
2. Evaluate the accuracy of each model on the inclined surface, by comparing the measured data with the predicted data.
3. Predict the solar radiation on the inclined surface, by modified solar radiation models with the Photographical Method.
4. Evaluate the accuracy of modified solar radiation models with the Photographical Method on an inclined surface.
5. Compare the accuracy of the existing solar radiation model with the modified solar radiation model by using the Photographical Method.

2. Solar radiation model

Global solar radiation on a surface can be divided into the following three components: (1) direct component, (2) sky diffuse component, and (3) ground-reflected component.

There are many prediction models that have been developed to predict accurate solar radiation on an inclined surface, according to variables such as latitude, longitude,

solar time, geometrical relationships, and climates. In this study, based on the previous researches, we evaluated the following five models that are relatively widely used, and that are known to be accurate.

2.1. The isotropic sky model

The isotropic sky model (Liu and Jordan, 1963) is the most common and simplest model. It assumes an all sky diffuse component that is uniformly radiated over the sky dome. It considers only the isotropic dome part, and the circumsolar brightening and horizon brightening parts are assumed to be zero. The ground-reflected component is calculated using global horizontal radiation, ground reflectance (albedo), and view factor to the ground. For a given tilted angle β (from the horizontal plane), the global solar radiation on an inclined surface is as follows:

$$I = I_{DN}\cos i + I_{dH}\,\mathrm{SVF} + I_{GH}\,\rho\,\mathrm{GVF} \quad (1)$$

(When $|i| > 90°$, $\cos i = 0$).

2.2. The Hay-Davies model

Hay and Davies (1980) developed an anisotropic model. It stands on the basis of the isotropic model, and reflects circumsolar brightening concentrated at the center of the sun. Horizon brightening that is concentrated at the horizon is not considered.

The isotropic sky model assumes that diffuse solar energy radiates 100% from the isotropic dome part, but this model considers that it radiates from just some of the isotropic dome part. For example, the circumsolar part is concentrated at the center of the sun. This circumsolar part assumes a direct solar radiation component. For this purpose, an anisotropic index K that represents the atmospheric transmittance for direct radiation has been proposed, as follows.

$$K = I_{DN}/I_O \quad (2)$$

For a given tilted angle β (from the horizontal plane) and K, the global solar radiation on an inclined surface is as follows:

$$I = I_{DN}\cos i + I_{dH}\{(1-K)\mathrm{SVF} + K\cos i\} + I_{GH}\,\rho\,\mathrm{GVF} \quad (3)$$

(When $|i| > 90°$, $\cos i = 0$).

2.3. The Reindl model

According to Reindl et al. (1990), the Hay and Davies model could not consider the horizon brightening part, and diffuse radiation on the surfaces is under-predicted. So they added the horizon brightening part to the Hay and Davies model.

They used the circumsolar part in the Hay and Davies model, and combined the horizon brightening correction factor from Klucher (1979). The global solar radiation on an inclined surface is as follows:

$$I = I_{DN}\cos i + I_{dH}\{(1-K)\mathrm{SVF}\times[1 + \mathrm{SQRT}(I_{dH}/I_{GH})\sin^3(\beta/2)] + K\cos i\} + I_{GH}\,\rho\,\mathrm{GVF} \quad (4)$$

(When $|i| > 90°$, $\cos i = 0$).

Diffuse radiation is calculated slightly higher than the Hay and Davies model. That is why only horizon brightening is added, and other components are unchanged.

2.4. The Perez model

The Perez model (Perez et al., 1990), which is used to estimate the solar radiation in the engine of EnergyPlus, DOE-2, TRNSYS-TUD and ESP-r, is more computationally intensive.

Perez et al. divided the sky diffuse component into the following three parts: the Isotropic dome part, Circumsolar brightening part, and Horizon brightening part (Fig. 1) (UIUC, 2011).

This model analyzes in detail the diffuse radiation, in the isotropic dome part, circumsolar brightening part and horizon brightening part. The circumsolar coefficient F_1, and horizon brightening coefficient F_2, empirically take the incidence angle of the sun and surface coefficients a, b into account, and they presented the following equation.

$$I = I_{DN}\cos i + I_{dH}\{(1-F_1)\mathrm{SVF} + F_1(a/b) + F_2 \times \sin\beta\} + I_{GH}\,\rho\,\mathrm{GVF} \quad (5)$$

(When $|i| > 90°$, $\cos i = 0$).

The coefficients are presented in their papers (Perez et al., 1987, 1990).

2.5. The Muneer model

The Muneer model (1990) integrates the background sky diffuse radiance into the anisotropic sky model. After researching on the shaded surface or the sunlit surface, he also distinguished the difference between the overcast condition, and the non-overcast condition. He proposed two equations of the slope solar radiation – one for the

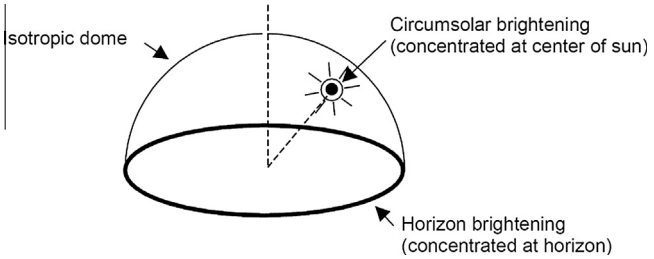

Fig. 1. Schematic view of the sky showing the solar radiance distribution as the superposition of three components.

shaded surface or the sunlit surface under an overcast sky, and the other one for the sunlit surface under a non-overcast sky.

For the shaded surface or sunlit surface under an overcast sky,

$$I = I_{DN}\cos i + I_{dH}T + I_{GH}\rho\,GVF \quad (6)$$

For the sunlit surface under a non-overcast sky

$$I = I_{DN}\cos i + I_{dH}[T(1-K) + K(\cos i/\sin\alpha)] + I_{GH}\rho\,GVF \quad (7)$$

$$T = 2SVF\{\cos^2(\beta/2) + [2R/\pi(3+2R)] \times [\sin(\beta) - \beta\cos(\beta) - \pi sin^2(\beta/2)]\} \quad (8)$$

(When $|i| > 90°$, $\cos i = 0$).

R is defined as the radiance distribution index of the sky brightness. Muneer described this index as a function of K. The function was obtained differently from fourteen locations worldwide (Muneer, 2004). We decided to choose the function for Japan for use in our study, as it is geographically closest to our region. And we also evaluated the Muneer model with the coefficients of southern Europe, to verify the applicability of PM in another region.

$$2R/\pi(3+2R) = 0.08000 - 1.050K - 2.8400K^2 \text{ (for Japan)} \quad (9)$$

$$2R/\pi(3+2R) = 0.00263 - 0.712K - 0.6883K^2 \text{ (for Southern Europe)} \quad (10)$$

3. Ground reflectance prediction model

A correct ground reflectance is essential, to predict the accurate solar radiation on surfaces. Ineichen et al. (1987) mentioned the importance of the appropriate ground reflectance, as follows.

> "A good evaluation of the reflected radiation is an essential complement to any diffuse radiation and daylight transposition model."

In recent years, the ground reflectance (albedo) of a specific region is directly measured by albedo meter. However, the albedos still have been calculated empirically, using latitude, position of the sun, climate, vegetarian and ground roughness. In this study, the following four albedo models were used (Liu and Jordan, 1963; Gueymard, 1993; Nkemdirim, 1972; Gueymard, 1987).

3.1. The isotropic constant model (ICM)

The most commonly used model is the Liu model (Liu and Jordan, 1963). This model was made using the measured data of Blue Hill, Massachusetts (latitude 42°14′N, longitude 71°07′W) from September, 1952 to August, 1956. Liu and Jordan proposed the ground albedo value monthly in a snowfall condition. A constant value of 0.2 was assumed for all months when the ground is covered with less than one inch of snow.

$$\rho = 0.2 \quad (11)$$

3.2. The isotropic seasonal model (ISM)

Gueymard (1993) calculated the ground albedo value as a function of latitude. He analyzed detailed seasonal maps of North America (Kung et al., 1964). The seasonal maps were made by using flight measurements for the whole region of North America, from Jan to Dec 1963. Using this data, he proposed a monthly average ground albedo calculation for $20 < Ø < 60$, as follows:

$$\rho = a_0 + a_1Ø + a_2Ø^2 + a_3Ø^3 \quad (12)$$

The monthly basis coefficients a_0, a_1, a_2, a_3 are presented in his paper (Gueymard, 1993). In our study, we calculated the ground albedo using latitude 37.6°, and obtained monthly ground albedo values.

3.3. The climatologically anisotropic model (CAM)

Nkemdirim (1972) proposed a climatologically anisotropic albedo model. He started his research on the basis of three concerns: (1) the relationship between albedo and zenith angle under different sky conditions; (2) the relationship between albedo and period of the day – forenoon and afternoon; and (3) the influence of irrigation on albedo. He undertook the experiment in the northwest of the University of Calgary campus (latitude 51°17′N, longitude 114°W, 1080 m MSL) on relatively flat prairie terrain, from June to September of 1971. He divided the experimental farm into four portions, and gave different conditions with vegetation or irrigation conditions. An equation was proposed based on the measurement data.

$$\rho = A\exp(B\theta_z) \quad (13)$$

The coefficients A and B are presented in his paper (Nkemdirim, 1972).

Psiloglou and Kambezidis (2009) estimated the ground albedo from other coefficients of A and B for Athens (latitude 37°59′N, longitude 23°45′ E, 107 m MSL). Athens's latitude is very similar to that of Korea (latitude 37°35'N). In this paper, Psiloglou and Kambezidis's coefficients of ($A = 0.198$, $B = 0.00804$) and ($A = 0.190$, $B = 0.00887$) were used for the period of morning and afternoon, respectively.

3.4. The semiphysical anisotropic model (SPAM)

Gueymard (1987) developed an anisotropic model to distinguish the albedo for direct and diffuse radiation. He calculated the albedo of direct and diffuse radiation, and derived global radiation reflectance with sky clearness. The average albedo for global irradiation is as follows:

$$\rho = f_{bs}\rho_b(1 - I_{dH}/I_{GH}) + \rho_d(I_{dH}/I_{GH}) \quad (14)$$

Where,

$$\rho_b = \rho_n + (f_{ab} + f_{af})|\cos\alpha| \exp[1.77 - 1.53H - 3.61H^2] \quad (15)$$

$$\rho_d = \rho_n + 0.023(f_{ab} + f_{af}) \quad (16)$$

ρ_b is the reflectance for direct radiation, and ρ_d is the reflectance for diffuse radiation. When the foreground is not horizontal, H can be replaced by $0.01(90° - i)$. The measuring field of our study is in an urban area, which is composed of half green grass and half concrete, and has no direct shading. The parameter values f_{ab} and f_{af} are calculated by the mean value of green grass and concrete, as 0.625 and 0.625, respectively. An input value of 1 is used as the Geuymard's shadow factor for direct solar radiation (f_{bs}). The ground reflectance for purely isotropic reflection ρ_n has been estimated as 0.171, with the usual albedo value of 0.2 (Liu and Jordan, 1963).

4. The Photographical Method

The sky view factor (SVF) and ground view factor (GVF) are required for the calculation of sky and ground diffuse components. They are calculated based on the surface inclined angle (β) in existing solar radiation models, and the equations are as follows:

$$SVF = (1 + \cos\beta)/2 \quad (17)$$

$$GVF = (1 - \cos\beta)/2 \quad (18)$$

But, the above values could not take into account the surrounding buildings and obstacles. In this study, we tried to find a way to consider the surroundings, which can affect the solar radiation on a surface. So, we proposed the Photographical Method (PM), by modifying the SVF and GVF, to consider the impact of the surroundings.

When calculating the SVF, the surrounding buildings and obstacles are assumed to be the ground in PM. So, SVF is not $(1 + \cos\beta)/2$, but the actual sky area ratio; and GVF is the ground area ratio (1-SVF), excepting the sky area ratio.

For modifying the SVF and GVF, we first took a picture of the same field of view with pyranometers installed on a slope, and analyzed the area ratio of the sky and the ground. The area ratio of the sky from the entire area of the picture is used as the view factor (SVF) of the sky diffuse radiation, and the area ratio of the ground is used as the view factor (GVF) of the ground-reflected radiation. This process provides a brief overview of the PM. Direct radiation is calculated simply by using the direct horizontal radiation and incidence angle. So, we excluded it from the scope of this study, and followed existing methods.

Fig. 2 is a photo taken from a vertical surface for calculating the SVF. We used a lens that has a 180° fish-eye angle of view, and appropriate body to the lens.

Fig. 2. View from the pyranometer for calculating the SVF.

When calculating the view factor with the conventional method of vertical surface ($\beta = 90°$), the SVF is 0.5 (=(1 + cos90)/2), and the GVF is 0.5 (=(1 − cos90)/2). However, as we can see in Fig. 2, the sky view predicted by the conventional method is shielding by trees and buildings (the brown part in Fig. 2 is the ground area calculated by the conventional method, and the blue part is the sky). So, it is hard to say that the SVF is 0.5. The solar radiation from the trees and buildings should be part of the ground-reflected radiation that is not part of the sky diffuse radiation. For more accurate prediction, we recalculated the SVF and GVF (see Fig. 3).

The SVF in an urban environment can be commonly derived by the following methods (Chen et al., 2012).

The first way is the analytical method, which can provide a theoretical equation for calculating the SVF for a particular point. Johnson and Watson (1984), and Oke (1987) used this method to calculate the SVF.

Another way to derive the SVF is the photographic method. This method uses a fish-eye lens, to project the hemispheric environment to a circular plane. It converts the color images to grey, and changes the brightness and contrast, to define the SVF. Anderson (1964), Barring et al. (1985), Steyn et al. (1986), and Clarke et al. (2008)used this method.

Yet another way is the GPS method. Chapman (Chapman et al., 2002; Chapman and Thornes, 2004) used this method to calculate the SVF directly from satellite data.

The last way is the software method. This method employs building a database like 3D models, GIS-data, and urban environment. Gal et al. (2009), Ratti and Richens (1999), Lindberg (2005), Rzepa (2009), and Grimmond et al. (2001) all suggested their own software for this method. Their various software methods are widely used now. Quite recently, Ivanova (2013) suggested an Anisotropic Factor that considers the anisotropic nature of sky diffuse radiance, and its change from the zenith to

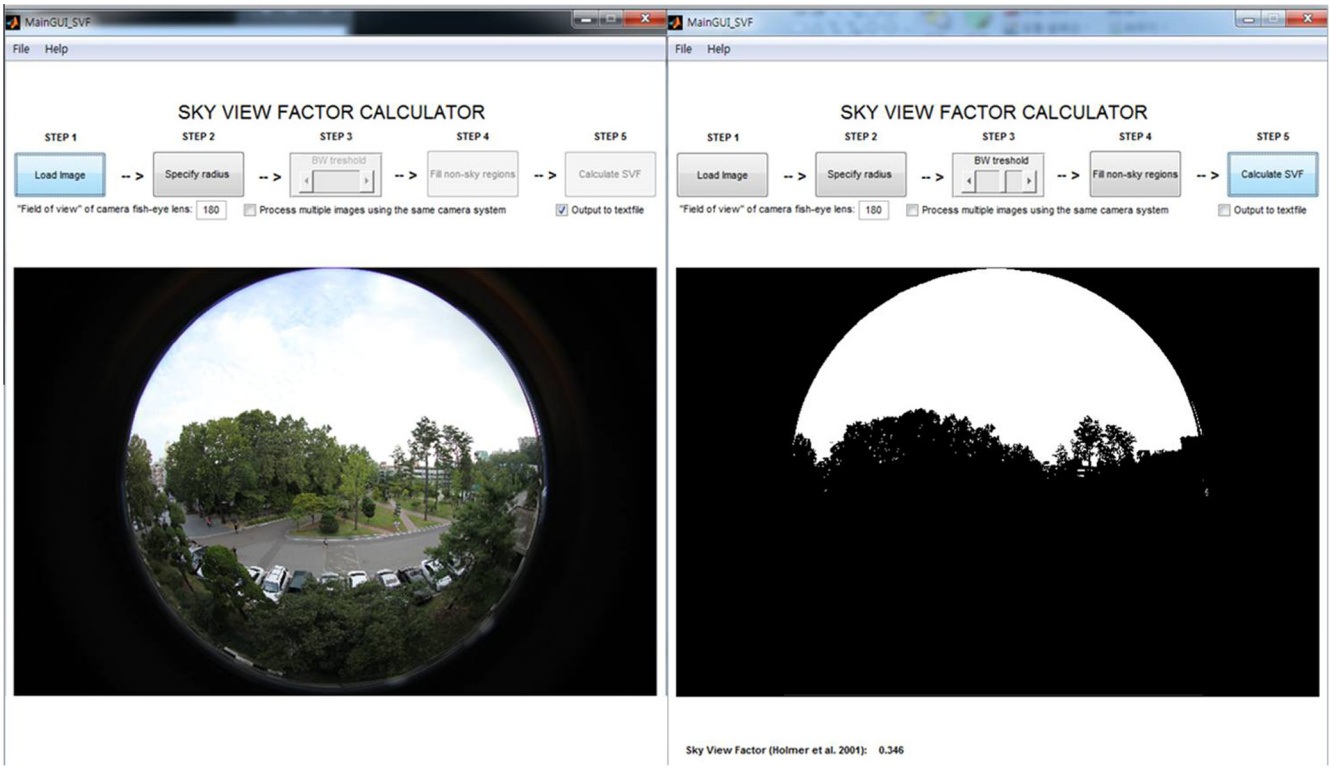

Fig. 3. The result of the sky view factor calculation software.

the horizon. For this paper we chose Holmer et al.'s software method (2001) to determine the SVF and GVF. This model is the pixel-based method, and the flow of the steps to calculate the SVF is as follows.

(1) Import a scanned fisheye image to the IDRISI.
(2) Calculate the image center, radius and corner.
(3) Create the pixel weight image.
(4) Delimit the fisheye image.
(5) Find the limit between sky and non-sky pixels.
(6) Assign the value 1 to all sky pixels, and 0 to all non-sky pixels.
(7) Multiply the images with each other.
(8) Sum the pixels, to calculate the SVF.

Holmer et al. mentioned the accuracy of this method. The accuracy of the SVF value is affected by the image thresholds and the pixel size. In their study, the error is less than 0.05 by applying thresholds of the fisheye images; and the error by the pixel size is less than 0.009.

In Fig. 3, from Holmer et al.'s software(Lindberg and Holmer, 2010), we found the SVF value of 0.346, and the GVF value of 0.654 (1-SVF). We evaluated the global solar irradiance on an inclined surface, by replacing the existing SVF with the calculated SVF with the PM, and analyzed the accuracy improvement.

Fig. 4 shows the flowchart calculating the global solar irradiance on an inclined surface with the PM.

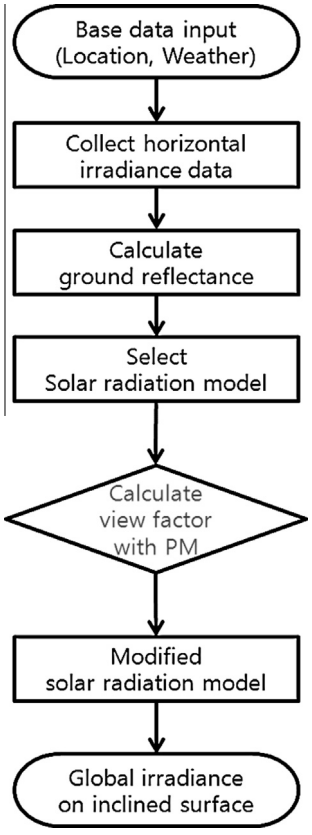

Fig. 4. Flowchart of the Photographical Method (PM).

5. Data collection

The data were collected at the Korea University of Seoul, Korea (Longitude 127°01' East, Latitude 37°35' North, elevation of 47 m above sea level).

The global horizontal radiation, diffuse horizontal radiation, and global radiation on an inclined surface were measured during the period from 22 June to 19 December, 2012 (7 am to 7 pm).

Global and diffuse horizontal radiations were measured on the roof of the test building. Two global radiations were measured on the wall of the building's fourth floor, and on an inclined surface (of 30° surface tilt angle) on the roof.

Fig. 5 shows the layout for the measurement system of the global horizontal radiation, diffuse horizontal radiation and global radiation on each surface. A digital camera (Cannon EOS 5D Mark II) with fish-eye was used to take pictures of the view from the pyranometers.

The global horizontal radiation, global vertical radiation and global radiation on the inclined surface were measured by LP PYRA 02 pyranometer, and diffuse radiation was measured by LP PYRA 12 pyranometer with shadow band. All instruments were First Class pyranometers, in accordance with ISO 9060. These pyranometers were calibrated, to ensure consistent measurements. We chose the latest pyranometer as the reference instrument. The pyranometers were calibrated from 5 to 7 June, 2012 (7 am to 7 pm), against the reference instrument.

The shadow band of a pyranometer can block both direct radiation, and a considerable portion of the diffuse radiation. The obscured diffuse solar radiation by shadow band has been corrected by using the Drummond isotropic model (Drummond, 1956). Solar radiation data were collected at an interval of one-minute, and the process is as follows:

- Remove the radiation data smaller than 1.0 W/m^2.
- Remove the datasets of greater diffuse horizontal values than the global horizontal values.
- Use the time-averaged values before and after a half hour.

The initial data consisted of 2158 h data collected during 166 days. From the data, we removed 579 hourly data, during the above-mentioned process.

6. Statistical results of hourly solar radiation on inclined surfaces

The measured data were analyzed with MBE and RMSE, which are typically used to evaluate the prediction accuracy of solar radiation. Analysis was performed based on the values of RMSE that can reflect the tendency of the individual data.

6.1. Analysis of the hourly solar radiation on a vertical surface by different twenty solar radiation prediction models

The prediction accuracy of the Photographical Method (PM) was compared with twenty existing different

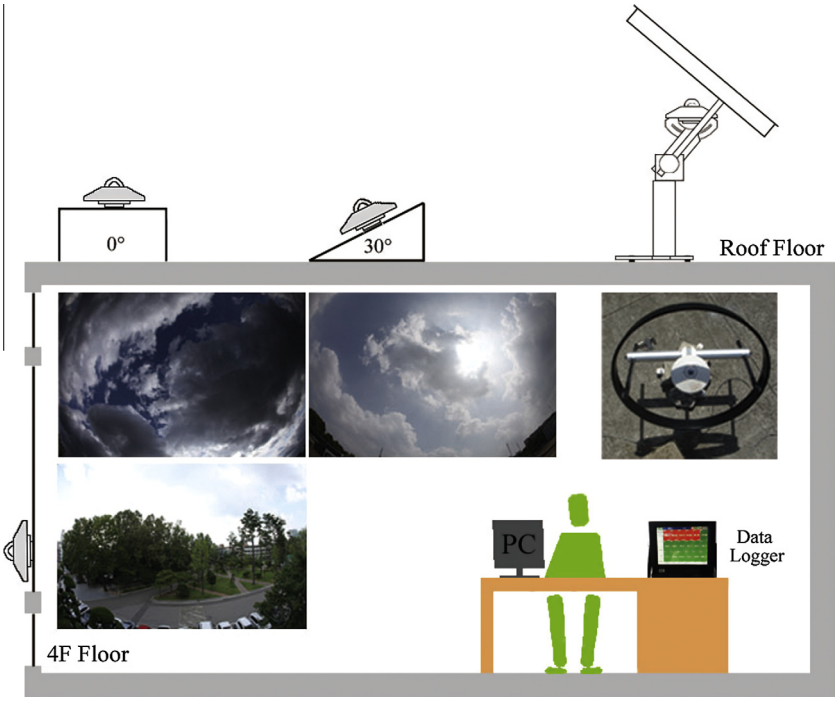

Fig. 5. Test cell with pyranometers, and view from the pyranometers of the global horizontal radiation, diffuse horizontal radiation and global radiation on an inclined surface.

Table 1
MBE and RMSE of hourly solar radiation on a vertical surface.

Albedo model	Solar radiation model	Symbol	Existing model		Modified model with PM	
			RMSE	MBE	RMSE	MBE
ICM	Isotropic	1–1	30	15	29	10
	Hay-Davies	1–2	34	19	34	15
	Reindl	1–3	65	29	65	24
	Perez	1–4	55	44	37	15
	Muneer	1–5	39	27	28	13
ISM	Isotropic	**2–1**	**29**	**12**	**29**	**6**
	Hay-Davies	**2–2**	**34**	**17**	**34**	**11**
	Reindl	**2–3**	**64**	**27**	**64**	**22**
	Perez	**2–4**	**53**	**42**	**37**	**12**
	Muneer	**2–5**	**35**	**23**	**27**	**9**
CAM	Isotropic	3–1	32	20	31	17
	Hay-Davies	3–2	36	24	36	21
	Reindl	3–3	64	32	64	29
	Perez	3–4	59	48	40	21
	Muneer	3–5	44	34	31	19
SPAM	Isotropic	4–1	30	15	29	10
	Hay-Davies	4–2	34	19	34	15
	Reindl	4–3	65	29	66	25
	Perez	4–4	56	44	38	16
	Muneer	4–5	39	28	28	13

prediction models of the global solar irradiance on an inclined surface. We measured the global radiations on a vertical surface (90° surface tilt angle) from 22 June to 14 October, and from 30 October to 19 December, 2012. The twenty prediction models were comprised of combinations of five radiation models and four albedo models. Table 1 shows the analyzed results of hourly radiation on an inclined surface, according to the different prediction models by RMSE and MBE.

Although the existing results were affected unevenly by the new method, all of the results have been properly enhanced. The improved prediction accuracy from the modified twenty models is shown in Fig. 6.

As shown in Fig. 6, the solar radiation models with ISM albedo model (case 2-1 to 2-5) have the most accurate predictability. The CAM albedo models (case 3-1 to 3-5) have a lower improvement than the ISM in accuracy. The ICM (case 1-1 to 1-5) and SPAM (case 4-1 to 4-5) showed similar accuracy, depending on the solar radiation model. In particular, the best RMSE values were revealed from the Isotropic and Muneer models with applying the PM. The best RMSE values are shown in boldface in Table 1. In almost all cases, the prediction accuracy showed an improvement with applying the PM.

All five solar radiation models were made from the measurement data in Europe and North America. The Isotropic and Hay models give relatively little influence to the region. The Muneer model provides a formula with measured data in Japan, which is close to Korea. But in the Reindl and Perez model, they used empirical formulas to

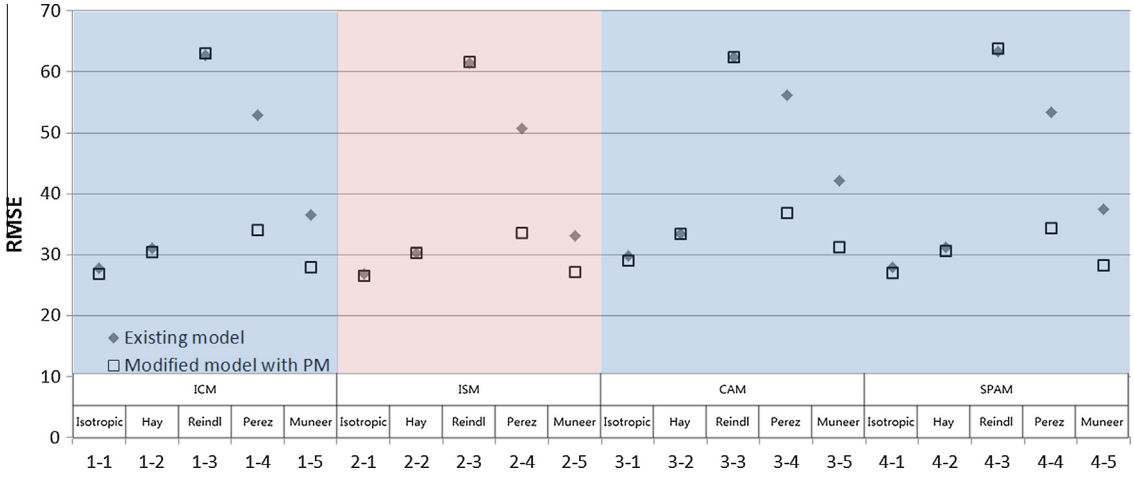

Fig. 6. Improvement of the accuracy of predicting solar radiation for the 20 cases (4 albedo models × 5 radiation models).

decide the coefficients. These empirical formulas can be affected by local weather conditions and vegetation. So, it may not be accurate in our region (Seoul, Eastern Asia). In practice, the statistical values of the Reindl model (RMSE: 64) and Perez model (RMSE: 37) showed relatively large values, compared to the values of the Isotropic model (RMSE: 29) and Muneer model (RMSE: 27). In particular, it can be said that the Reindl model is not suitable in Seoul, because of its large RMSE value of 64 (MBE: 22). The Isotropic model that employed the simplest method showed the best statistical values (RMSE: 29, MBE: 6). Many factors could not guarantee better prediction accuracy, and there is a suitable prediction model according to the characteristics of the region. Based on the data from the measurement period, the Isotropic model is the best suitable prediction model in the studied region.

Figs. 7 and 8 show a comparison between the measured solar radiation, and the calculated solar radiation (Right-hand: modified model with the PM). Fig. 7 shows the most accurate prediction combination of the ISM and Isotropic models (improved from 12 to 6 of MBE with the same RMSE value). Fig. 8 shows the best accuracy improvement after combination of the ISM and Perez models (improved from 53 to 37 of RMSE and from 42 to 12 of MBE). These values can also be found in Table 1.

In this study, the surrounding buildings and obstacles were assumed to be a uniform ground. But, additional studies about the type, shape and reflectance of the obstacles are needed, in order to obtain more accurate results. For further verification, we also evaluated the Muneer model with the coefficients of southern Europe, to verify the applicability of the PM in another region. We verified the improvement of prediction accuracy of the solar radiation after applying the PM, and the results are shown in Appendix Fig. A.1.

The results revealed that the rate of improvement of the prediction accuracy could be more improved in the low range of solar radiation (high proportion of diffuse solar radiation), with application of the PM.

6.2. Analysis of the hourly solar radiation on an inclined surface, according to the proportion of diffuse radiation

To analyze the accuracy improvement according to the proportion of diffuse horizontal solar radiation, we defined the I_{dH}/I_{GH} ratio as three ranges of 0.8–1.0, 0.2–0.8 and 0–0.2. Table 2 shows the accuracy improvement, according to the variation of I_{dH}/I_{GH}. The high range of 0.8–1.0 contains about 51% of the entire data. The middle range of 0.2–0.8 has 42% of the data. 7% of the data are included in the range of 0.0–0.2.

Table 2 shows the accuracy improvement according to the proportion of the diffuse radiation (I_{dH}/I_{GH}). In existing models, the worst prediction model reveals the value of RMSE as 242 in the range of 1.0–0.8; the best prediction model is in the range of 0–0.2, with the RMSE of 34 (see Fig. 9).

After the application of PM, the two statistical indicators were improved in all ranges of I_{dH}/I_{GH}. In particular, the best improvement was achieved by reducing the RMSE from 242 to 71, in the range of 0.8–1.0 (see Fig. 10).

The Photographical Method considers the actual ground view factor of the ground-reflected component, and the sky view factor of the sky diffuse component, in the global solar radiation. It is difficult to expect accuracy improvement by applying the PM when the direct component is dominant, because the direct component is calculated with the conventional method. Therefore, when the percentage of diffuse radiation (the sky diffuse and ground-reflected component) is higher, the prediction accuracy has largely improved by the PM. The degree of accuracy improvement of predictability by the portion of diffuse radiation for all cases has been added to the appendix.

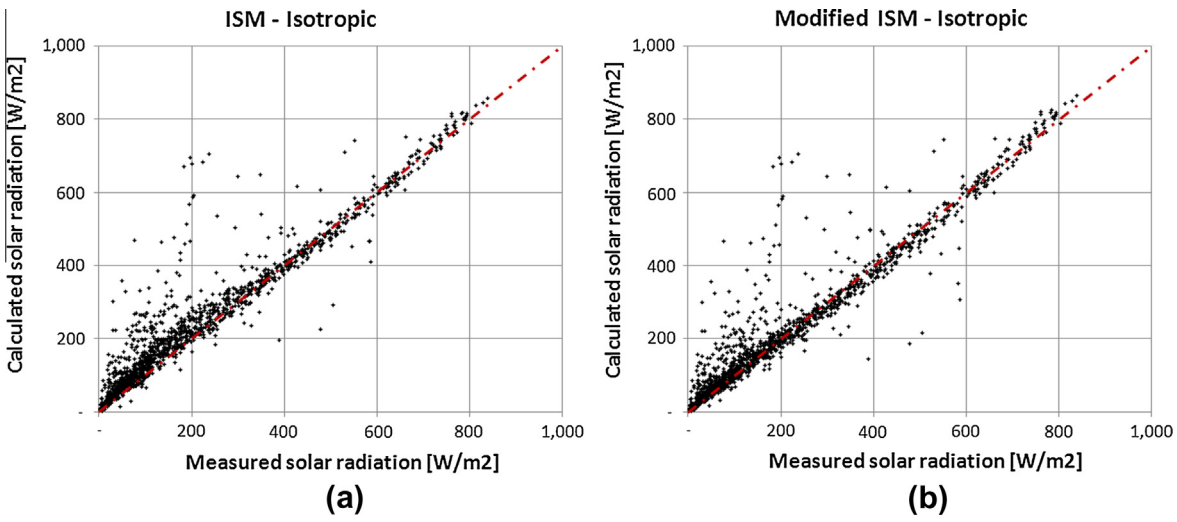

Fig. 7. Calculated and measured hourly solar radiation on a vertical surface for: (a) combination of the ISM and existing Isotropic model, and (b) combination of the ISM and modified Isotropic model with the PM.

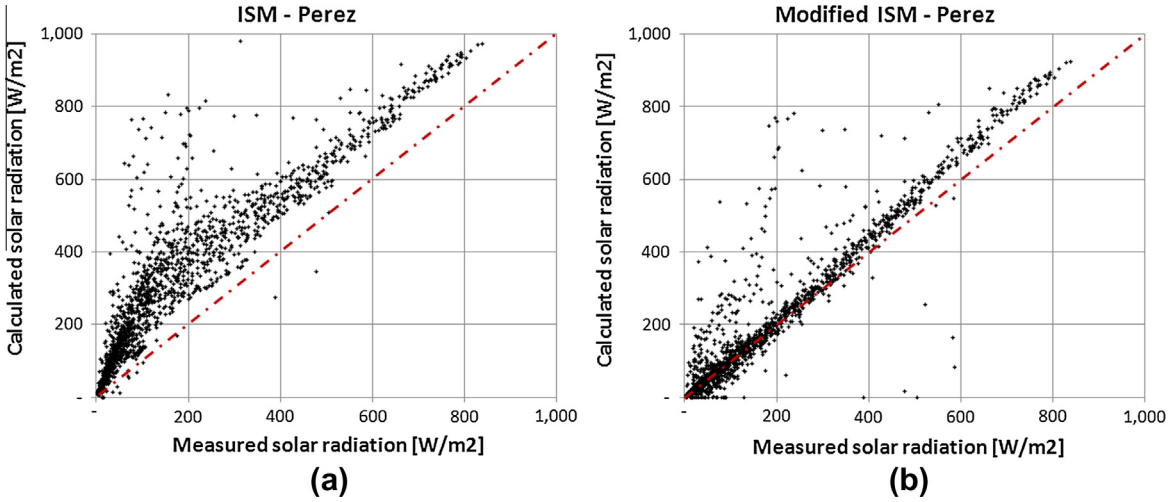

Fig. 8. Calculated and measured hourly solar radiation on a vertical surface for: (a) combination of the ISM and existing Perez model, and (b) combination of the ISM and modified Perez model with the PM.

Table 2
Prediction accuracy of the solar radiation on a vertical surface, according to the proportion of the diffuse horizontal radiation with the existing and modified Perez models.

ISM-Perez	I_{dH}/I_{GH}	Existing model	Modified model with PM	Improvement ratio (%)
MBE	1.00–0.81	171	−2	98.7
	0.80–0.21	54	17	68.7
	0.20–0.00	28	18	37.1
RMSE	1.00–0.81	242	71	70.8
	0.80–0.21	62	34	45.0
	0.20–0.00	34	26	22.2

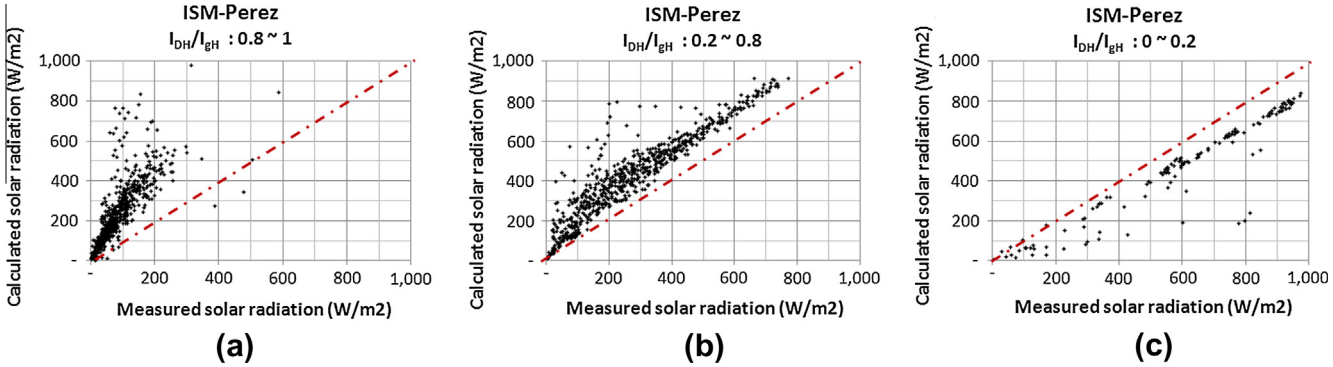

Fig. 9. Measured and calculated solar radiation on an inclined surface for combination of the ISM and existing Perez models, according to the proportion of horizontal diffuse radiation (a) from 0.8 to 1, (b) from 0.2 to 0.8, and (c) from 0 to 0.2.

6.3. Analysis of the hourly solar radiation on another surface inclination

To assess the applicability of PM on another surface inclination, a pyranometer was mounted on the floor of the building's roof, to collect solar radiation data on an inclined surface (30° surface tilt angle, 0° azimuth angle). The measured data were collected from 15 October to 22 October, 2012. We analyzed the measured data versus calculated data with the existing ISM-Perez model, and then compared the data with those of the modified ISM-Perez-PM model. We evaluated the accuracy improvement of predicting the solar radiation, after applying the PM.

Fig. 11 shows the view from the pyranometer on an inclined surface (the brown part in Fig. 11 is the ground area calculated by the conventional method, and the blue part is the sky area). The SVF calculated with the conventional method was 0.933, but this value was changed to 0.895 after applying the PM. Fig. 12 shows the accuracy improvement after applying the PM. The accuracy improvement is better in a high proportion of diffuse horizontal solar radiation, but the improvement in accuracy is not noticeable over that of the PM with vertical surface.

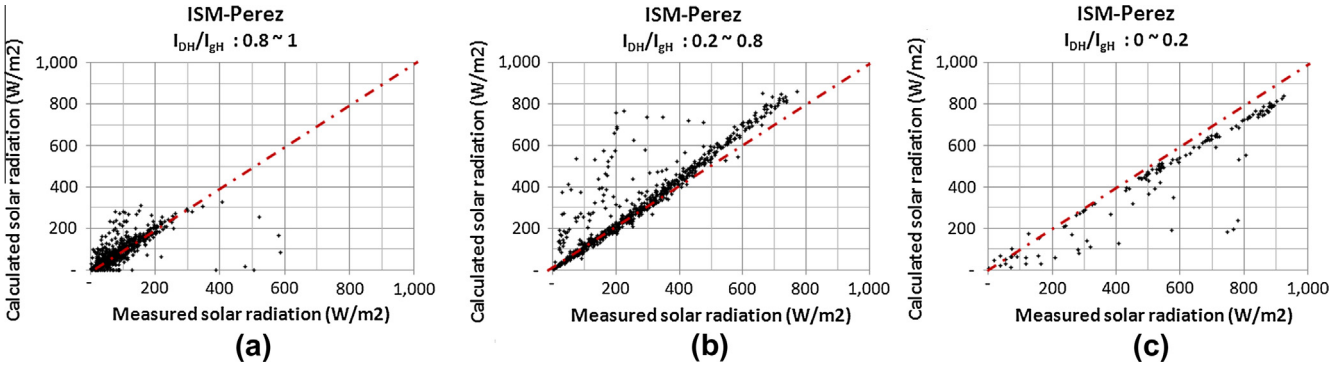

Fig. 10. Measured and calculated solar radiation on an inclined surface for combination of the ISM and modified Perez models, according to the proportion of horizontal diffuse radiation (a) from 0.8 to 1, (b) from 0.2 to 0.8, and (c) from 0 to 0.2.

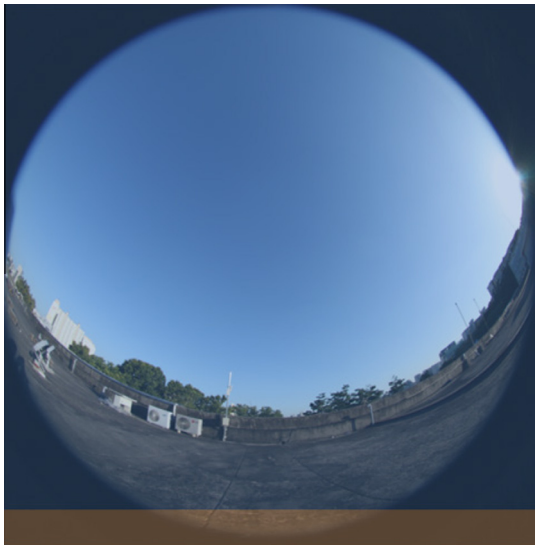

Fig. 11. View from the pyranometer installed on the south surface ($\beta = 30°$).

With an increasing surface inclination value, there can be many obstacles affecting the solar radiation on the normal direction of the slope. So the calculated solar radiation with conventional process can hold large errors with various environments. The results of this study show that the PM can effectively correct these errors.

On the other hand, the expected accuracy improvement by applying the PM could be decreased with a low surface inclination range.

Table 3 shows the accuracy improvement according to the proportion of the diffuse horizontal radiation (I_{dH}/I_{GH}), with surface inclinations β of 90 degrees and 30 degrees.

The degree of accuracy improvement of 30 degree surface inclination is relatively lower, than the degree of accuracy improvement of higher degree of surface inclination; and sometimes, the values are rather worse.

In existing models, the worst case is under 0.8–1.0 of I_{dH}/I_{GH}, and the value of RMSE was 53; and the best prediction model is under 0–0.2 of I_{dH}/I_{GH}, and the value of RMSE was 11. After the application of PM, two statistical indicators were improved, under the range of 0.8–1.0 and 0.2–0.8. It was not improved under the range of 0–0.2.

The PM has a lesser improvement of prediction accuracy in the range of smaller surface tilt angle. With applying the PM, the SVF of a vertical surface changed from 0.5

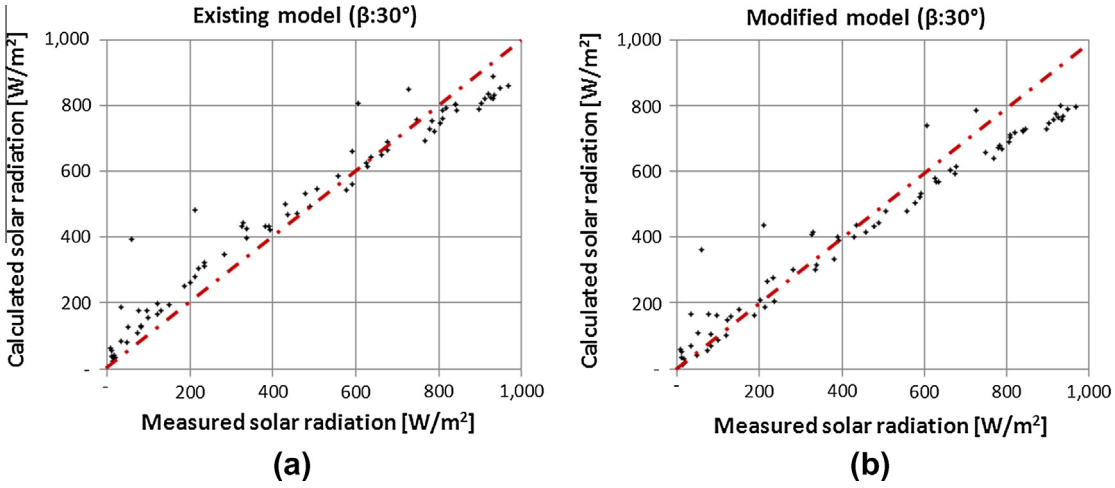

Fig. 12. Calculated and measured hourly solar radiation on an inclined surface for: (a) a combination of the ISM and existing Perez model, and (b) a combination of the ISM and modified Perez model with the PM.

Table 3
Prediction accuracy of solar radiation on an inclined surface with the existing and modified Perez models, with surface inclinations β of 90° and 30°.

	I_{dH}/I_{GH}	$\beta = 90°$		$\beta = 30°$	
		Existing model (SVF = 0.5)	Modified model with PM (SVF = 0.346)	Existing model (SVF = 0.933)	Modified model with PM (SVF = 0.895)
MBE	1.00–0.81	171	−2	47	−8
	0.80–0.21	54	17	15	0
	0.20–0.00	28	18	−4	−12
RMSE	1.00–0.81	242	71	53	20
	0.80–0.21	62	34	25	24
	0.20–0.00	34	26	11	16

to 0.346. In the case of an inclined surface ($\beta = 30°$), the SVF was changed from 0.933 to 0.895.

A modified SVF with the PM is important, to predict the solar radiation on an inclined surface

7. Discussion and conclusion

A new method was proposed to predict the solar radiation on an inclined surface in the urban city. To evaluate the usefulness of the Photographical Method, we evaluated twenty cases (5 solar radiation models for each of 4 albedo models), and the following conclusions were drawn:

1. When applying the PM, the accuracy of prediction of the solar radiation on an inclined surface was improved in all twenty cases. In particular, the Perez model showed the greatest improvement.
2. The diffuse solar radiation ratio was used to inspect the accuracy of the PM with various radiation conditions. In all cases, a higher ratio of diffuse horizontal solar radiation showed a better improvement of prediction accuracy. When the diffuse solar radiation ratio was higher than 80%, the accuracy of prediction was improved a lot. The MBE improved from 171 to -2, and the RMSE improved from 242 to 71 in the Perez model. However when the diffuse solar radiation ratio was lower than 20%, the prediction accuracy was merely improved from 28 to 18 for the MBE, and 34 to 26 for the RMSE. The proposed method does not consider the direct radiation, but is concerned with the view factor of the sky diffuse radiation and ground-reflected radiation, only. Therefore, the prediction accuracy of diffuse radiation has been improved; however, the prediction accuracy of direct radiation has not been improved.
3. With increasing the tilt angle from the horizon to the vertical, the modified model showed better prediction accuracy of the solar radiation. The PM is well reflective of the influence of obstacles against the solar radiation on a surface. When the surface tilted

Table A.1
The MBE and RMSE of hourly solar radiation on a vertical surface, according to the proportion of the diffuse horizontal radiation with the existing and modified models.

	Existing model						Modified with PM					
I_d/I_g	1.0–0.81	0.8–0.21	0.2–0.0	1.0–0.81	0.8–0.21	0.2–0.0	1.0–0.81	0.8–0.21	0.2–0.0	1.0–0.81	0.8–0.21	0.2–0.0
Symbol	MBE			RMSE			MBE			RMSE		
1-1	40	14	9	65	28	21	18	9	10	48	26	21
1-2	46	20	14	72	35	25	20	17	16	51	34	26
1-3	61	46	7	98	85	45	32	41	9	69	81	45
1-4	183	61	31	258	69	37	6	22	20	72	36	28
1-5	61	34	24	94	43	30	12	14	27	37	23	44
2-1	34	10	7	59	27	20	10	5	8	45	25	20
2-2	40	16	12	66	34	24	12	12	14	48	32	24
2-3	54	42	5	90	82	44	24	36	7	62	77	44
2-4	171	54	28	242	62	34	−2	17	18	71	34	26
2-5	49	28	21	79	37	28	5	10	23	33	21	42
3-1	50	20	14	75	31	23	31	18	17	57	30	24
3-2	57	26	19	82	39	28	34	25	23	60	39	30
3-3	71	52	12	108	88	45	46	49	16	80	85	47
3-4	204	74	42	280	81	46	19	30	27	76	42	33
3-5	82	47	35	116	54	39	26	22	36	45	28	50
4-1	40	14	9	65	28	21	18	10	10	48	26	21
4-2	46	20	14	72	35	25	20	17	16	51	34	26
4-3	61	46	7	98	86	45	32	42	9	70	83	46
4-4	183	62	31	258	70	37	6	22	20	72	36	28
4-5	61	36	24	95	45	30	13	14	27	38	23	45

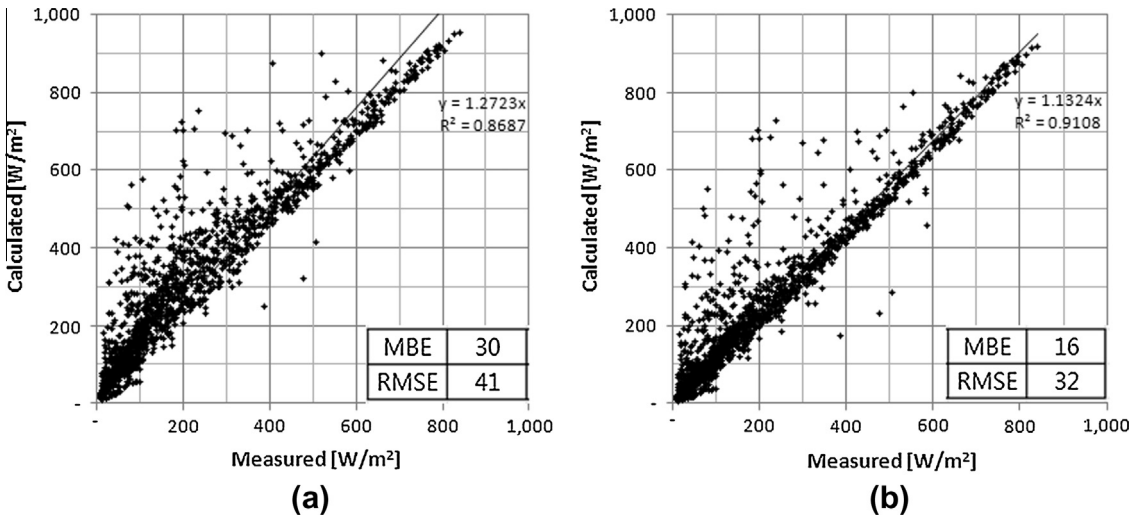

Fig. A.1. The results of the hourly solar radiation on a vertical surface with the ISM-Muneer model, after applying the coefficients for Southern Europe.

angle is increased, there are many surrounding obstacles, which can be assumed as ground. With increase of the area of obstacles from the sky view, the prediction accuracy can be greatly improved by the new method.

The PM is more useful to predict solar radiation in an urban region with forests of buildings, than in a region of wide grasslands with sunny climate.

For a large tilted surface, the estimated radiation can be changed by the photo point. To make up the error, we can employ the SVF value from the center point of the large surface, as a representative value. The researcher can take the mean value, by dividing the surface into several parts. If information were to be available about the building, it would also be possible to derive the fisheye-view, by using a virtual reality-based 3D modeling application.

Acknowledgements

This research was supported by the Basic Science Research Program, through the National Research Foundation of Korea (NRF), funded by the Ministry of Education, Science and Technology (NRF-2013R1A1A2A10005456).

Appendix A. Appendix

Table A.1 is a result of the statistical analysis of the hourly solar radiation on a vertical surface, according to the proportion of the diffuse horizontal radiation with the PM, for all cases. Although there are differences in prediction accuracy, in most cases, the accuracy has been improved with the PM.

The coefficients for Southern Europe$2R/\pi(3+2R) = 0.00263–0.712K–0.6883K^2$

The statistical results are all improved, after applying the PM. The MBE value improved from 30 to 16, and the value of the RMSE improved from 41 to 32. The PM can be applicable to Muneer's equation with the coefficients of Southern Europe. The PM can be used, with using the coefficients of other regions (see Fig. A.1).

References

Anderson, M.C., 1964. Studies of the Woodland light climate: I. The photographic computation of light conditions. J. Ecol. 52, 27–41.

Barring, L., Mattsson, J.O., Lindqvist, S., 1985. Canyon geometry, street temperatures and urban heat island in Malmo, Sweden. J. Climatol. 5, 433–444.

Chapman, L. et al., 2002. Sky-view factor approximation using GPS receivers. Int. J. Climatol. 22, 615–621.

Chapman, L., Thornes, J.E., 2004. Real-time sky-view factor calculation approximation. J. Atmos. Oceanic Technol. 21, 730–742.

Chen et al., 2012. Sky view factor analysis of street canyons and its implications for daytime intra-urban air temperature differentials in high-rise, high-density urban areas of Hong Kong: a GIS-based simulation approach. Int. J. Climatol. 32, 121–136.

Clarke, P. et al., 2008. Models for the estimation of building integrated photovoltaic systems in urban environments. Proc. Inst. Mech. Eng., Part A: J. Power Energy 1, 61–67.

Cucumo, M. et al., 2007. Experimental testing of models for the estimation of hourly solar radiation on vertical surface at Arcavacata di Rende. Sol. Energy 81, 692–695.

Diez-Mediavilla, M. et al., 2005. Measurement and comparison of diffuse solar irradiance models on inclined surfaces in Valladolid (Spain). Energy Convers. Manage. 46, 2075–2092.

Drummond, A.J., 1956. On the measurement of sky radiation. Arch. Meteor. Geophys. Bioklim. B 7, 413–436.

El-Sebaii, A.A. et al., 2010. Global, direct and diffuse solar radiation on horizontal and tilted surfaces in Jeddah, Saudi Arabia. Appl. Energy 87, 568–576.

Gal, T. et al., 2009. Computing continuous sky view factors using 3D urban raster and vector databases: comparison and application to urban climate. Theoret. Appl. Climatol. 95, 111–123.

Grimmond, C.S.B. et al., 2001. Rapid methods to estimate sky-view factors applied to urban areas. Int. J. Climatol. 21, 903–913.

Gueymard, C., 1987. An anisotropic solar irradiance model for tilted surfaces and its comparison with selected engineering algorithms. Sol. Energy 38, 367–386.

Gueymard, C., 1993. Mathematically integrable parameterization of clear sky beam and global irradiances and its use in daily irradiation applications. Sol. Energy 50, 385–397.

Hay, J.E., Davies, J.A., 1980, Calculation of the solar radiation incident on an inclined surface. In: Proceedings First Canadian Solar Radiation Data Workshop, pp. 59–72.
Holmer, B. et al., 2001. Sky view factors in forest canopies calculated with IDRISI. Theoret. Appl. Climatol. 68, 33–40.
Ineichen, P. et al., 1987. The importance of correct albedo determination for adequately modeling energy received by tilted surfaces. Sol. Energy 39, 301–305.
Ivanova, S.M., 2013. Estimation of background diffuse irradiance on orthogonal surfaces under partially obstructed anisotropic sky. Part I – Vertical surfaces. Sol. Energy 95, 376–391.
Johnson, G.T., Watson, I.D., 1984. The determination of view factors in urban canyons. J. Climate Appl. Meteorol. 2, 329–335.
Kambezidis, H.D. et al., 1994. Measurements and models for total solar irradiance on inclined surface in Athens, Greece. Sol. Energy 53, 177–185.
Klucher, T.M., 1979. Evaluation of models to predict insolation on tilted surface. Sol. Energy 23, 111–114.
Kung, E.C., Bryson, R.A., Lenschow, D.H., 1964. Study of a continental surface albedo on the basis of flight measurements and structure of the earth's surface cover over North America. Mon. Weather Rev. 92, 543–564.
Lindberg, F., 2005. Towards the use of local governmental 3-D data within urban climatology studies. Mapping Image Sci. 2, 32–37.
Lindberg, F., Holmer, B. 2010. Sky View Factor Calculator User Manual – Version 1.1. University of Gothenburg.
Liu, B.Y.H., Jordan, R.C., 1963. The long term average performance of flat plate solar energy collectors. Sol. Energy 7, 53–74.
Loutzenhiser, P.G. et al., 2007. Empirical validation of models to compute solar irradiance on inclined surfaces for building energy simulation. Sol. Energy 81, 254–267.
Muneer, T., 1990. Solar radiation model for Europe. Build. Services Eng. Res. Technol. 11, 153.
Muneer, T., 2004. Solar radiation and Daylight Models, second ed. Elsevier Butterworth Heinemann.
Nkemdirim, L.C., 1972. A note on the albedo of surfaces. J. Appl. Meteorol. 11, 867–874.
Oke, T.R., 1987. Boundary Layer Climates, second ed., Methuen.
Perez, R. et al., 1987. A new simplified version of the Perez diffuse irradiance model for tilted surfaces. Sol. Energy 39, 221–231.
Perez, R. et al., 1990. Modeling daylight availability and irradiance components from direct and global irradiance. Sol. Energy 44, 271–289.
Psiloglou, B.E., Kambezidis, H.D., 2009. Estimation of the ground albedo for the Athens area, Greece. J. Atmos. Solar Terr. Phys. 71, 943–954.
Ratti, C., Richens, P., 1999. Urban texture analysis with image processing techniques. Paper presented at CAAD Futures 99. Atlanta, GA.
Reindl, D.T. et al., 1990. Evaluation of hourly tilted surface radiation models. Sol. Energy 45, 9–17.
Rzepa, M., 2009. The map of sky view factor in the center of Lodz. Paper presented at the 7th International Conference on Urban Climate. Yokohama, Japan 29.
Steyn, D.G. et al., 1986. The determination of sky view-factors in urban environments using video imagery. J. Atmos. Oceanic Technol. 3, 759–764.
UIUC, LBNL, 2011. EnergyPlus Engineering Reference: the Reference to EnergyPlus Calculations, U.S. Department of Energy.
Vartiainen, Eero., 2000. A new approach to estimating the diffuse irradiance on inclined surfaces. Renewable Energy 20, 45–64.